Articles

Journal of Avian Biology 46: 528–537, 2015
doi: 10.1111/jav.00590

Subject Editor: Jan-Åke Nilsson. Editor-in-Chief: Thomas Alerstam. Accepted 16 March 2015

Uncommon paleodistribution patterns of *Chrysolophus* pheasants in east Asia: explanations and implications

Nan Lyu, Martin Päckert, Dieter Thomas Tietze and Yue-Hua Sun

Y.-H. Sun (sunyh@ioz.ac.cn) and N. Lyu, Key Laboratory of Animal Ecology and Conservation Biology, Inst. of Zoology, Chinese Academy of Sciences, Beijing 100101, PR China. – M. Päckert, Senckenberg Naturhistorische Sammlungen, Museum für Tierkunde, Königsbrücker Landstraße 159, DE-01109 Dresden, Germany. – M. Päckert, Biodiversity and Climate Research Center (BiK–F), Senckenberganlage 25, DE-60325 Frankfurt am Main, Germany. – D. T. Tietze, Inst. of Pharmacy and Molecular Biotechnology, Heidelberg Univ., Im Neuenheimer Feld 364, DE-69120 Heidelberg, Germany.

Some modeling studies indicated that the past distributions of species in east Asia during the Last Interglacial (LIG) and Last Glacial Maximum (LGM) periods differ from those of European and North American species and the deviant Asian distribution pattern is known under the term 'pre-LGM expansion'. It represents the unusually similar distribution patterns between the current and the LGM scenario. However, there is still no satisfying explanation for this phenomenon so far. Therefore, we took the two recently separated pheasant species of genus *Chrysolophus* in east Asia as an example to test the pattern by performing ecological niche models. The main findings of this study include: 1) the paleodistributions of these two pheasants also corresponded to the 'pre-LGM expansion' pattern; 2) climatic similarity results from mobility-oriented parity analysis also revealed similar pattern for both species; 3) climate regimes of east Asia showed patterns different from those in Europe and North America in a climate shift towards drier conditions and stronger seasonality and to more extreme temperatures of the coldest months particularly during the LIG; 4) the two *Chrysolophus* species occupied significantly different ecological niches according to current distribution. We suggest that ecological segregation established in allopatric glacial refugia should be the main determinants for the separation of two *Chrysolophus* species until they came into extant post-Pleistocene contact.

Pleistocene climate fluctuations were demonstrated to entail significantly geographical distribution shifts and contractions of species (Hewitt 2000). Modeling studies assessing the Pleistocene distributions of European and North American species revealed that the current geographical distribution of many species were rather similar to those reconstructed for the Last Interglacial period (LIG) 0.13–0.07 mya (Levsen et al. 2012, Wilson and Pitts 2012). In contrast, the ranges of most species had contracted into smaller, fragmented and low-latitudinal refuges during the Last Glacial Maximum (LGM) 0.021–0.018 mya (Waltari et al. 2007, Lait et al. 2012, Manthey et al. 2012, Lait and Burg 2013).

Species from other parts of the globe, particularly those of east Asia, have so far attracted less attention from distribution modelers (Beheregaray 2008). Recent studies have indicated that the LIG and LGM distributions of east Asian bird species showed unusually similar distribution patterns between the current and the LGM scenario (Dai et al. 2011, Qu et al. 2011, Zhao et al. 2012, Sun et al. 2014, Ye et al. 2014). Recently, this phenomenon was termed 'pre-LGM expansion' (Wang et al. 2013) and it has received further support from studies of phylogeography and demographic history of SE Asian species (Li et al. 2006, Huang et al. 2010, Wang et al. 2013, Sun et al. 2014, Ye et al. 2014).

Nevertheless, the past distributions in those studies were mainly interpreted in order to explain lineage diversification and historical demography of target species in combination with genetic sequence data but no reasonable explanations for these uncommon distribution patterns were provided. There are two potential explanations for the east Asian pre-LGM expansion. Firstly, the unique climate of the region could have directly resulted in different species distributions, e.g. if the climate in this region was not as cold as in North America or Europe during the LGM period, some species could still live here rather than retreating southward. Alternatively, if local distributions have been influenced by species-specific niche preferences (Hewitt 2000), e.g. cold climate tolerance (Lu et al. 2012b), the uncommon distribution pattern may show even if the east Asian climates have been similar to other parts of the world.

The influence of Pleistocene climate fluctuations on species distributions and patterns of intraspecific genetic variation have attracted much attention (Hewitt 1996). Comparison of extant and past scenarios using ecological niche models (ENM) (Svenning et al. 2011) could provide

evidence of past disjunct distributions and provide important insight into how Pleistocene climate fluctuations drive speciation (Dincă et al. 2011, Levsen et al. 2012). Actually, using ENM for extrapolating the potential distributions of species during the past time should be generally based on the assumptions of climatic-niche stability through time and species–climate already equilibrium (Nogués-Bravo 2009). Although those assumptions are still under debate, ENMs using abundant occurrence data and limited-dimensional environment predictors (Peterson 2011) can potentially provide new insights into the ecological aspects of the evolutionary history of species (Kozak et al. 2008). Furthermore, there are approaches which can improve the use of ENMs for such extrapolation, such as quantifying the differences between the spaces for constructing ENMs and projecting (Elith and Leathwick 2009).

In this study, we explore the paleodistributions of two east Asian pheasant species belonging to the genus *Chrysolophus*: the golden pheasant *C. pictus* and Lady Amherst's pheasant *C. amherstiae*. Both species are native to the mountain forests of east Asia and they differ obviously in feather proportions and plumage color patterns (Lei and Lu 2006). Split ages estimates inferred from molecular data differ with respect to molecular markers and dating methods applied but generally hint to a mid- to late-Pleistocene origin with earliest separation times at 1.7 mya (Zhang et al. 1991, Xiangyu et al. 2000).

Here we attempt to test the pre-LGM expansion hypothesis for east Asian species using the two *Chrysolophus* pheasants as a case study. We also explore the niche divergences of them by comparing the distributions of current and past scenarios and measuring the niche differentiation quantitatively. Moreover, since past distributions should be related to climates at that time, assessments of climatic characteristics may provide reasonable and direct explanations for the uncommon LGM and LIG distribution patterns in east Asia. Therefore, we assess the climatic similarities between current and past situations for both species using the mobility-oriented parity (MOP) analysis (Owens et al. 2013), and then calculate the differences of climatic layers amongst three timeframes to find an explanation for the uncommon 'pre-LGM expansion' pattern in east Asia.

Material and methods

Ecological niche modeling

We applied a maximum entropy algorithm (MaxEnt, ver. 3.3.3.k) to construct the species specific ENMs and to predict the potential current, LGM and LIG distributions of both *Chrysolophus* pheasants (Phillips et al. 2006, Phillips and Dudík 2008). We obtained 262 and 146 occurrence records for *C. pictus* and *C. amherstiae*, respectively, from the literature, museum records (provided by the National Zoological Museum of China) and the Global Biodiversity Information Facility (GBIF, <www.gbif.org>). Several records did not have geographic coordinates, and we assigned coordinates using the description of the localities and Google Earth 5.0 (Google, Mountain View, CA, USA; <http://earth.google.com>). In order to minimize any sampling bias effect (Potts et al. 2013a, b), we resampled localities to ensure that all occurrence records were separated from each other by at least 0.1° (Wang et al. 2013). This resulted in 232 localities for *C. pictus* and 120 for *C. amherstiae* (Fig. 1). To reduce the uncertainty of the model predictions, ENM calibrations should be restricted to a certain accessible area (Anderson and Raza 2010, Barve et al. 2011). Therefore, we calibrated the ENMs within a moderate study region limit, selecting a 200-km buffer around each occurrence point (VanDerWal et al. 2009) for each species (Fig. 1) to allow for possible presence locations beyond known boundaries. As ground

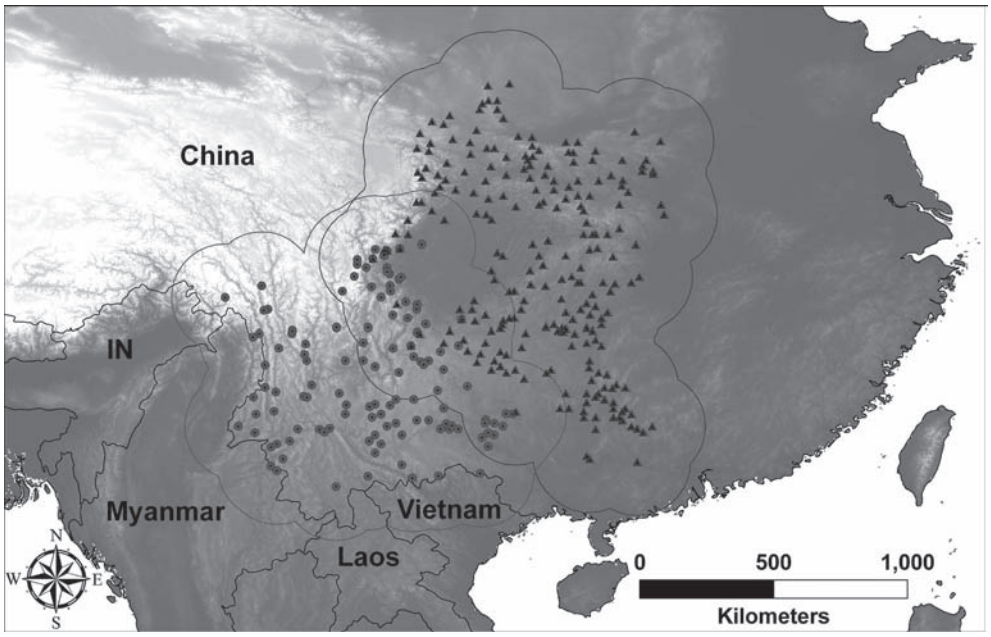

Figure 1. Occurrence records of *Chyrsolophus pictus* (black triangles) and *C. amherstiae* (grey dots). The areas within the polygons were used to construct the ENMs; the whole area shown here was used to project the current, LGM and LIG distributions.

living birds, both pheasants show similarly limited capabilities for long-distance flight, and mainly glide across the small open areas according to field observations (Lei and Lu 2006). Therefore, the movement distance of individuals is unlikely to be larger than 200-km. Thus, the use of such study region should be appropriate.

We assessed model robustness for each ENM analysis by selecting cross-validation with five replicates (Phillips et al. 2006). The importance of different predictors was examined using a Jackknife analysis of the regularized gain with training data (Phillips et al. 2006), that is 80% of the total data. The logistic output was selected with suitability values ranging from 0 to 1 (Phillips and Dudík 2008), with other settings set as default, e.g. convergence threshold (10^{-5}) and maximum number of iterations (500). The final predicted suitability outputs of different ENMs were obtained through averaging the five replicates (Marmion et al. 2009). Model performance was assessed by calculating the area under the curve (AUC) of receiver operating characteristics (ROC; Fielding and Bell 1997) and the true skills statistics (TSS; Allouche et al. 2006) using the function 'presence.absence.accuracy' in the R package 'PresenceAbsence' (Freeman and Moisen 2008). Since absence data were not available, AUC and TSS values only represent the ability of ENMs to distinguish presence data from the background rather than absence (Phillips et al. 2006). Prior to calculation, we generated 1000 random pseudo-absences (Elith et al. 2006) using the function 'randomPoints' of the R package 'dismo' (Hijmans et al. 2011). All accuracy assessments were conducted using R ver. 2.14.1 (R Development Core Team).

Climatic layers and predictor selection

We used 19 bio-climatic layers with a spatial resolution of 2.5 arc-minutes, from the WorldClim database (Hijmans et al. 2005, Supplementary material Appendix 1, Table A1) to construct the ENMs and predicting species distributions (Peterson et al. 2006, Lu et al. 2012a). To assess the importance of predictor selection (Peterson and Nakazawa 2008), we constructed ENMs using two kinds of predictor sets for comparison and ensemble prediction (Araújo and New 2007). First, we used all 19 bio-climatic layers as predictors to construct the full model (FULL) and then calculated a Pearson's correlation matrix for all 19 data layers. Depending on the importance of each layer derived from Jackknife analysis of the FULL model Supplementary material Appendix 1, Fig. A1, a correlation coefficient threshold of 0.85 (Elith et al. 2006) was used to determine whether each layer was to be included or removed from the model. The remaining layers were used to construct an uncorrelated model (UNCOR) for both species (Supplementary material Appendix 1, Table A1).

Projected past distributions

In order to avoid reduced transferability capacity of ENMs (Peterson et al. 2007, Jiménez-Valverde et al. 2011), we used the projected outputs of UNCOR model with reduced uncorrelated variables to assess the LGM and LIG distributions of both species. Prior to developing projections for past distributions, we extracted the same reconstructed climatic variables of LGM and LIG for east Asia. LGM climatic data layers were obtained from two general atmospheric circulation models: the community climate system model (CCSM) and the model for interdisciplinary research on climate (MIROC). The original LGM data sets were downloaded from the Paleoclimate Modeling Intercomparison Project Phase II (PMIP2) through WorldClim (< www.worldclim.org >). LIG climatic data sets were based on models from Otto-Bliesner et al. (2006), which were also available from WorldClim. In order to test the reliability of projected distributions, we applied the MOP analysis (Owens et al. 2013) to assess the climatic similarity between current calibration of each species and projected region during LIG and LGM. As a modification and extension of original multivariate environmental similarity surface (MESS) (Elith et al. 2010), MOP analysis can identify strict extrapolation areas and give similarity values ranging from 0 to 1 (Owens et al. 2013).

Niche overlap assessment

Predicted outputs of the MaxEnt models were used to assess niche overlap and divergence of both *Chrysolophus* species using ENMtools (ver. 1.3; Warren et al. 2008, 2010). Niches were compared based on Schoener's *D* (Schoener 1968) and Warren's *I* (Warren et al. 2008). Both metrics measure the similarity between predictions of habitat suitability of species, which range from 0 (no niche overlap) to 1 (complete niche overlap). We used the niche identity test to determine whether the ENMs generated for the two species were significantly (ecologically) different (Warren et al. 2008). We obtained a null distribution from 100 pseudo-replicates by pooling and randomizing the occurrence points throughout the study regions of both species to construct simulated ENMs, each of which had the same number of points as the target species. Significance assessment was performed using a one-tailed t-test with a confidence level of 0.05. We also conducted the background similarity test in ENMtools to determine whether the ENM of either species was more similar than expected by chance (Warren et al. 2010). This analysis calculates the values of *D* and *I* between a focal species and a set of null-niches modeled from pseudo-replicated data randomly sampled within the background range where the focal species occur (Warren et al. 2008). The sampling size was the same as the other species. Significance assessment was performed using a two-tailed t-test with a confidence level of 0.05, since it was possible that the niches of focal species are either more or less similar than the null ones. Furthermore, in order to examine the robustness of niche divergence of the two *Chrysolophus* species (Shaner et al. 2015), we tested the niche differences at various spatial scales of < 50 km, < 100 km, < 150 km and < 200 km of the contact zone using discriminant function analyses (DFA). Finally, we calculated the mean elevation of suitable areas of three timeframes (current, LGM and LIG) using ArcGIS ver. 9.3.1 (ESRI, Redlands, USA) based on the assumption that the elevation of the study area has not changed during the past 140 ka. The suitable areas were identified firstly using two presence thresholds of sensitivity – specificity minimizer (SSMIN) and sensitivity + specificity maximizer (SSMAX) as suggested by Jiménez-Valverde and Lobo (2007). Subsequently, only the areas with positive values of climatic similarity

Table 1. Accuracy assessment of two types of ecological niche model (ENM) for *Chrysolophus pictus* and *C. amherstiae*. FULL: ENM constructed using all bio-climatic layers as predictors; UNCOR: ENM constructed using the uncorrelated layers; AUC = area under relative operating characteristic curves; TSS = true skill statistic.

Species	ENM	TSS	AUC
C. pictus	FULL	0.56	0.84
	UNCOR	0.50	0.81
C. amherstiae	FULL	0.56	0.85
	UNCOR	0.52	0.82

indicated by MOP analysis (i.e. outside the strict extrapolation areas) were considered as suitable.

Climate assessments in east Asia

First, we comprehensively assessed the climatic similarities between current and past situations according to the outputs of the MOP analysis (Owens et al. 2013). Second, in order to provide visual illustrations of climatic differences in east Asia compared to other parts of the world, we calculated the differences of climatic predictor layers between current and LGM, current and LIG and LGM and LIG conditions. Specifically, five new layers were generated for each climatic layer through calculating the differences using ArcGIS, i.e. current minus CCSM, current minus MIROC, current minus LIG, LIG minus CCSM and LIG minus MIROC.

Results

Modeling accuracy assessment

Accuracy measurements revealed that both the FULL and UNCOR models were good fits for both *C. pictus* and *C. amherstiae* (Table 1). TSS values were ≥ 0.5 and the AUC values were > 0.80, indicating good predictive accuracies of those ENMs. The FULL model performance was only a slightly better fit than the UNCOR model due to higher values of both TSS and AUC (Table 1). Moreover, the correlation coefficients of the current outputs predicted by the two ENMs were 0.966 for *C. pictus* and 0.978 for *C. amherstiae*.

Current, LGM and LIG distributions

Our ENMs clearly identified that suitable areas of *C. pictus* habitat were located north of the northeastern range limits of *C. amherstiae* (Fig. 2). Overlap among suitable areas for both species was quite limited and confined to areas located in the western Sichuan Basin (Fig. 2c). The MOP analysis revealed that the most suitable areas of both species projected throughout east Asia were located within the regions having relatively larger values of similarity (Fig. 2a, b). Predicted past distributions indicated a history of dramatic range shifts for both species over the last 140 ka (Fig. 3). Generally, the distributions of suitable areas of both species during LGM were consistent with the results of the MOP analysis (Fig. 3). However, quite a large size of suitable areas during the LIG was identified as strict extrapolation (marked by ellipses in Fig. 3), and therefore those overlapped suitable areas shown in Fig. 3 should be treated with caution. The most suitable areas of *C. pictus* during the LIG were restricted to the mountains in Guizhou, northern Yunnan and India, while *C. amherstiae* was restricted primarily to Yunnan, Sichuan, Vietnam, eastern Laos and western Myanmar (Fig. 3). During the LGM, suitable areas for both species were predicted to have expanded eastwards and northwards compared to the LIG scenario (Fig. 3). Current distribution patterns were more similar to the LGM scenario rather than to the LIG scenario (Fig. 2 and 3, Supplementary material Appendix 1, Table A2). Furthermore, note that *C. pictus* had a large refugial area in Guizhou during the LIG that was almost completely isolated from the areas suitable for *C. amherstiae* (Fig. 3). The unsuitable areas between them were also identified as strict extrapolation by the MOP analysis (marked by arrow in Fig. 3).

Niche divergence between *C. pictus* and *C. amherstidae*

Niche overlap measures for *C. pictus* and *C. amherstiae* were $I = 0.356$ and $D = 0.153$, which were significantly lower when compared to the pseudo-replicates produced by the identity test (t-test, $p < 0.001$, Fig. 4a). This implies that the two *Chrysolophus* species occupy quite different ecological niches. The background similarity test also revealed that in either scenario of *C. pictus* versus *C. amherstiae* or *C. amherstiae* versus *C. pictus*, the actual niche overlap was significantly lower than the pseudo-replicates (t-test, $p < 0.001$, Fig. 4b, c). This suggested that the divergent niches between the two *Chrysolophus* species should not be due to the available climate spaces. Furthermore, the Jackknife results of UNCOR models revealed that temperature seasonality (BIO4) and precipitation seasonality (BIO15) contained

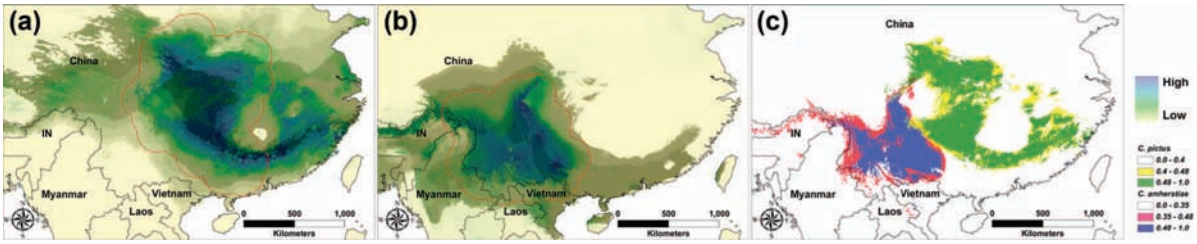

Figure 2. Projected current distributions of *Chrysolophus pictus* and *C. amherstiae* using the UNCOR model: (a) habitat suitability for *C. pictus*; (b) habitat suitability for *C. amherstiae*; (c) overlap of suitable areas identified using two kinds of threshold (SSMIN represents the threshold of sensitivity – specificity minimizer, while SSMAX represents the threshold of sensitivity + specificity maximizer). The areas with grey background in (a) and (b) have positive values of similarity calculated using MOP analysis. Higher similarities are shown by darker grey color. The suitable areas indicated as strict extrapolation are excluded in (c).

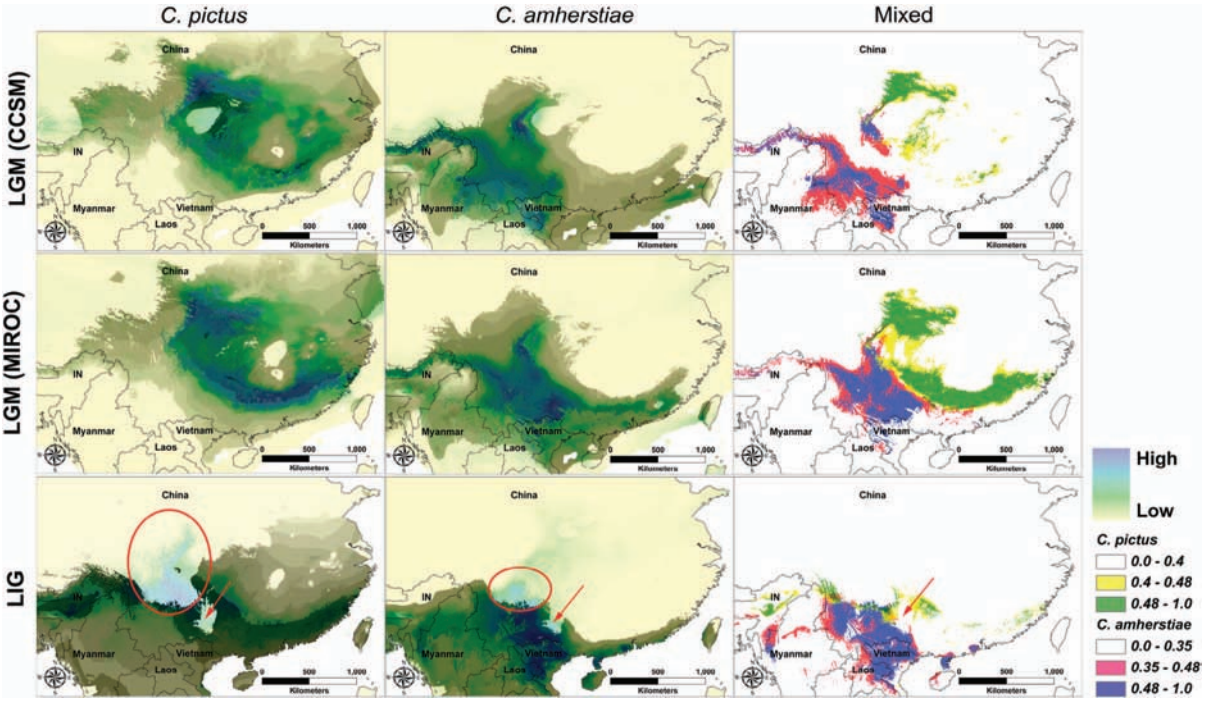

Figure 3. Projected LGM (CCSM and MIROC) and LIG distributions of *Chrysolophus pictus* and *C. amherstiae* using the UNCOR model. The first two columns show the habitat suitability distributions of the two species under different timeframes. The third column shows the overlap of suitable areas identified using the thresholds of SSMIN and SSMAX. The areas with grey background have positive values of similarity calculated using MOP analysis. Higher similarities are shown by darker grey color. The suitable areas indicated as strict extrapolation are excluded in the third column.

the most useful niche information for *C. pictus*, achieving the highest training and testing gains when used in isolation, whereas mean temperature of driest quarter (BIO9) and precipitation of coldest quarter (BIO19) contained the most useful niche information for *C. amherstiae*. According to the discriminant-function analysis, one canonical function including six variables (BIO3, BIO4, BIO7, BIO15, BIO17 and BIO19) was used in the analysis ($R^2 = 0.882$, $F_{6, 345} = 202.37$, $p < 0.001$) by applying a stepwise method. Generally, the canonical function score was significantly lower for *C. pictus* using all the presence data (t-test, $p < 0.001$, Fig. 5). The difference in function scores between the two species also showed persistence at different spatial scales as shown in Fig. 5. The current mean elevation of the areas suitable for *C. pictus* was lower than that of the areas suitable for *C. amherstiae* (Table 2). Moreover, the mean elevation of *C. amherstiae* showed a general increase from the LIG via the LGM to current, while the mean elevation of *C. pictus* during the LIG was the highest among the three timeframes.

Climate assessments

According to the MOP analysis, we found that the distributions of climatic similarities during the LGM for both species were quite similar to the current situations, while the areas with similar climate during the LIG were shown to shift southwards and westwards (Fig. 2 and 3). Furthermore, the current climate was generally warmer than the climate during the LGM throughout the globe, but especially in northern regions (indicated as darker blue color in Fig. 6a). Although the current annual mean temperature (BIO1) was lower than during the LIG in the even more northern areas (indicated as yellow color in Fig. 6a), larger areas in the south still had higher temperatures than during the LIG, i.e. with blue color in Fig. 6a. Moreover, the mean LIG temperature of some areas in southern and eastern Asia was even lower than during the LGM (Fig. 6a). Throughout the globe, the current annual precipitation (BIO12) was generally higher than the precipitation during the LGM, but was lower in eastern China (Fig. 6b). On the contrary, the annual precipitation during the LIG was lower than the current climate value and the value during the LGM scenario throughout eastern China. The precipitation of the wettest (BIO13) and driest months (BIO14) also showed similar patterns with annual precipitation (Supplementary material Appendix 1, Fig. A2).

While considering the layers about variation of temperature and precipitation, we found that either temperature (BIO4) or precipitation seasonality (BIO15) was more different between today and the LIG than between today and the LGM (Fig. 7). Furthermore, these layers about variation also showed some patterns in east Asia. Specifically, temperature seasonality values during the LIG were generally greater than those for both the LGM and the current period throughout Eurasia (Fig. 7a). Nonetheless, the areas in more southern Asia had relatively smaller difference values of BIO4 compared to the northern areas (Fig. 7a). Precipitation seasonality showed a pattern of LIG > LGM > current in southern and eastern Asia, which was consistent with Europe and North America (Fig. 7b). Nonetheless, the difference values of BIO15 in these areas were relatively smaller

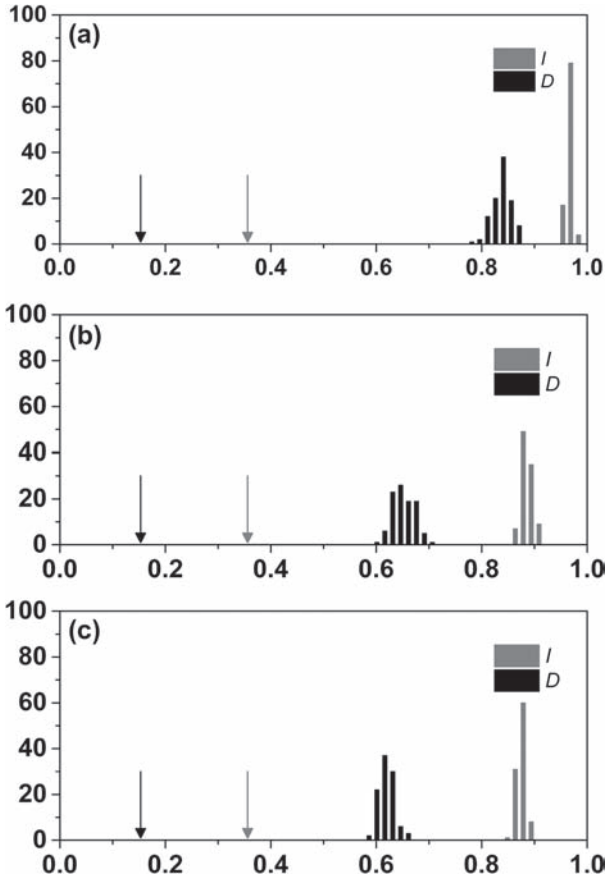

Figure 4. Identity test and background-similarity test results. Vertical arrows in the panel represent the observed niche similarity between occurrence points for the corresponding pair of both *Chrysolophus* species. The histograms represent the distribution of niche similarities obtained from pairs of pseudo-niches constructed by random resampling. (a) Identity test; (b) background-similarity test (*C. pictus* versus *C. amherstiae*); (c) background-similarity test (*C. amherstiae* versus *C. pictus*).

than in the areas of central and western China and some areas in Sichuan Province (Fig. 7b), suggesting that although the precipitation during the LIG was relatively lower than during the other periods in east Asia, monthly variation

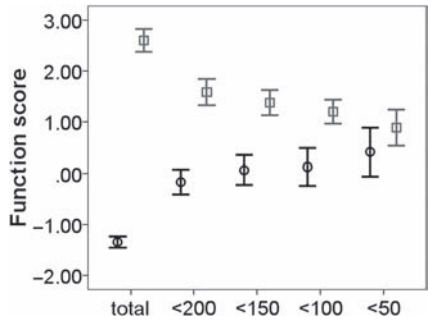

Figure 5. The canonical function scores of both *Chrysolophus* species at different scales of the contact zone. The mean canonical function scores of *C. pictus* and *C. amherstiae* are shown by the black and grey color, respectively. The error bars denote 95% confidence limits. The scores of *C. amherstiae* are generally higher than those of *C. pictus* at different scales (t-test, total: $p < 0.001$; < 200 km: $p < 0.001$; < 150 km: $p < 0.001$; < 100 km: $p < 0.001$; < 50 km: $p = 0.091$).

Table 2. Mean elevations of distribution ranges of *Chrysolophus pictus* and *C. amherstiae* for different timeframes under two kinds of threshold in meters (mean ± SD). SSMIN represents the threshold of sensitivity – specificity minimizer, while SSMAX represents the threshold of sensitivity + specificity maximizer.

Climate scenario	Threshold	*C. amherstiae*	*C. pictus*
Current	SSMIN	1886 ± 668	756 ± 539
	SSMAX	1951 ± 804	751 ± 569
LGM (CCSM)	SSMIN	1708 ± 778	1111 ± 579
	SSMAX	1737 ± 842	947 ± 564
LGM (MIROC)	SSMIN	1672 ± 714	710 ± 483
	SSMAX	1720 ± 860	734 ± 506
LIG	SSMIN	1340 ± 792	1461 ± 1041
	SSMAX	1300 ± 792	1361 ± 932

within any given year was also relatively smaller than the northern areas in China, which may enable the endemic species to survival in these areas.

Discussion

Niche divergence of *Chrysolophus* pheasants

Our ENMs outputs revealed that any overlap of potential suitable areas for both species was quite limited and restricted to the western and southern boundary of the Sichuan Basin. The species also differ in their elevational range preferences with *C. pictus* preferring lower elevations (Table 2). Note that the elevation is most strongly correlated to the mean temperature of the coldest quarter (BIO11), minimal temperature of coldest month (BIO6) and mean temperature of the driest quarter (BIO 9) with coefficients larger than 0.9. We can conclude that the major potential suitable areas of *C. pictus* would have largely unsuitable elevation and climates for *C. amherstiae* and vice versa. Specifically, temperature seasonality (BIO4) and precipitation seasonality (BIO15) contained most of the niche information of *C. pictus*, and the response curves showed that this species was more adapted to an environment with moderate temperature variation among seasons and lower variation in precipitation among months. On the contrary, the mean temperature of the driest quarter (BIO9) and the precipitation of the coldest quarter (BIO19) were the most significant predictor variables for *C. amherstiae*. The response curves showed that *C. amherstiae* prefers an environment with lower temperature of the driest quarter and moderate precipitation of the coldest quarter. Furthermore, the niche divergence of these two pheasants is relatively robust according to the DFA results at different scales of the contact zone (Fig. 5).

LGM and LIG climates in east Asia

Both the projected past distributions using ENMs and climatic similarity assessed from the MOP analysis (Fig. 3) showed that *C. pictus* and *C. amherstiae* displayed the pattern of 'pre-LGM expansion' (Wang et al. 2013). To date, there is no comprehensive explanation for this phenomenon, except that Wang et al. (2013) suggested that pre-LGM expansion may be related to a generally warmer climate

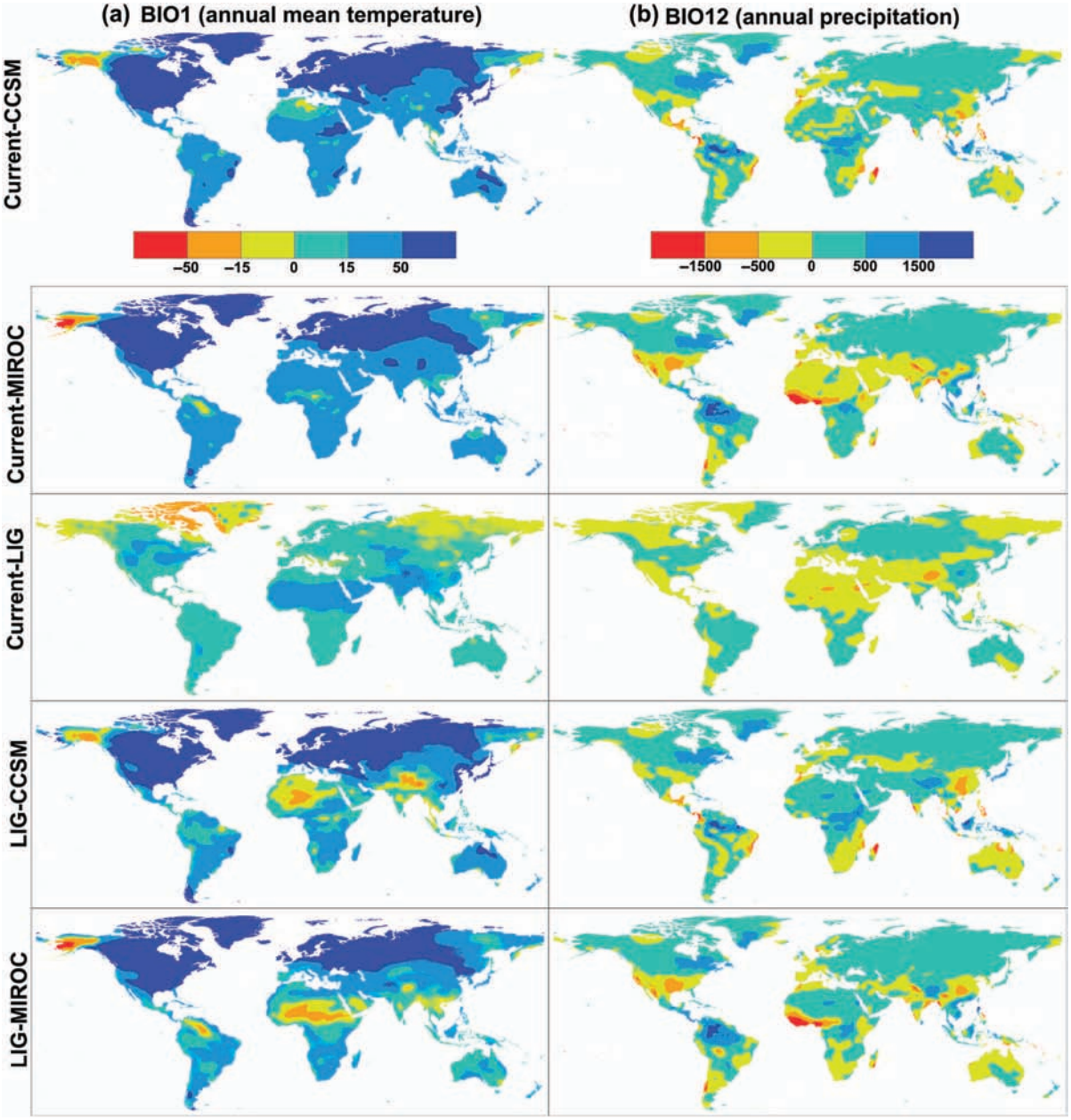

Figure 6. Climatic differences among three timeframes of current, LGM (under two atmospheric circulation models CCSM and MIROC) and LIG. Annual mean temperature (a) and annual precipitation (b) are shown. The values indicated here equal the values of each climate variable in the first scenario minus the second one (i.e. blue shades = climate variable higher in the first scenario than in the second one, and yellow/red shades = climate variable lower in the first scenario than in the second one).

during the LIG, compelling some montane species to occupy higher elevations (Colwell et al. 2008). In this study, we also calculated the degree of elevational shift in both pheasant species among three timeframes, but found that *C. amherstiae* demonstrated a surprising shift toward lower elevations during both the LGM and the LIG, when compared to the current geographical distribution. Therefore, a presumed warmer climate during the LIG compelling upward elevation range shifts cannot explain the distribution patterns for every species.

Our analyses revealed that the east Asian LGM and LIG climates differed from other regions of the same latitude around the globe in either the mean or variation values of temperature and precipitation (Fig. 6 and 7). Specifically, we found that some southern and western areas in Asia even had lower temperatures during the LIG than during the LGM (Fig. 6). One major reason for the deviating climate and distribution scenarios in SE Asia is the exposure of this region at the southeastern margin of the Qinghai-Tibet Plateau (QTP). Despite an ongoing debate on paleoclimatic scenarios most scientists agree that at latest from the late Miocene on the uplift of the plateau dramatically changed the regional climate with the onset of the SE Asian monsoon and its intensification during the Pliocene (An et al. 2001, Guo et al. 2008, Favre et al. 2014; Fig. 3). Along with global Pliocene cooling, three successive final uplift phases from

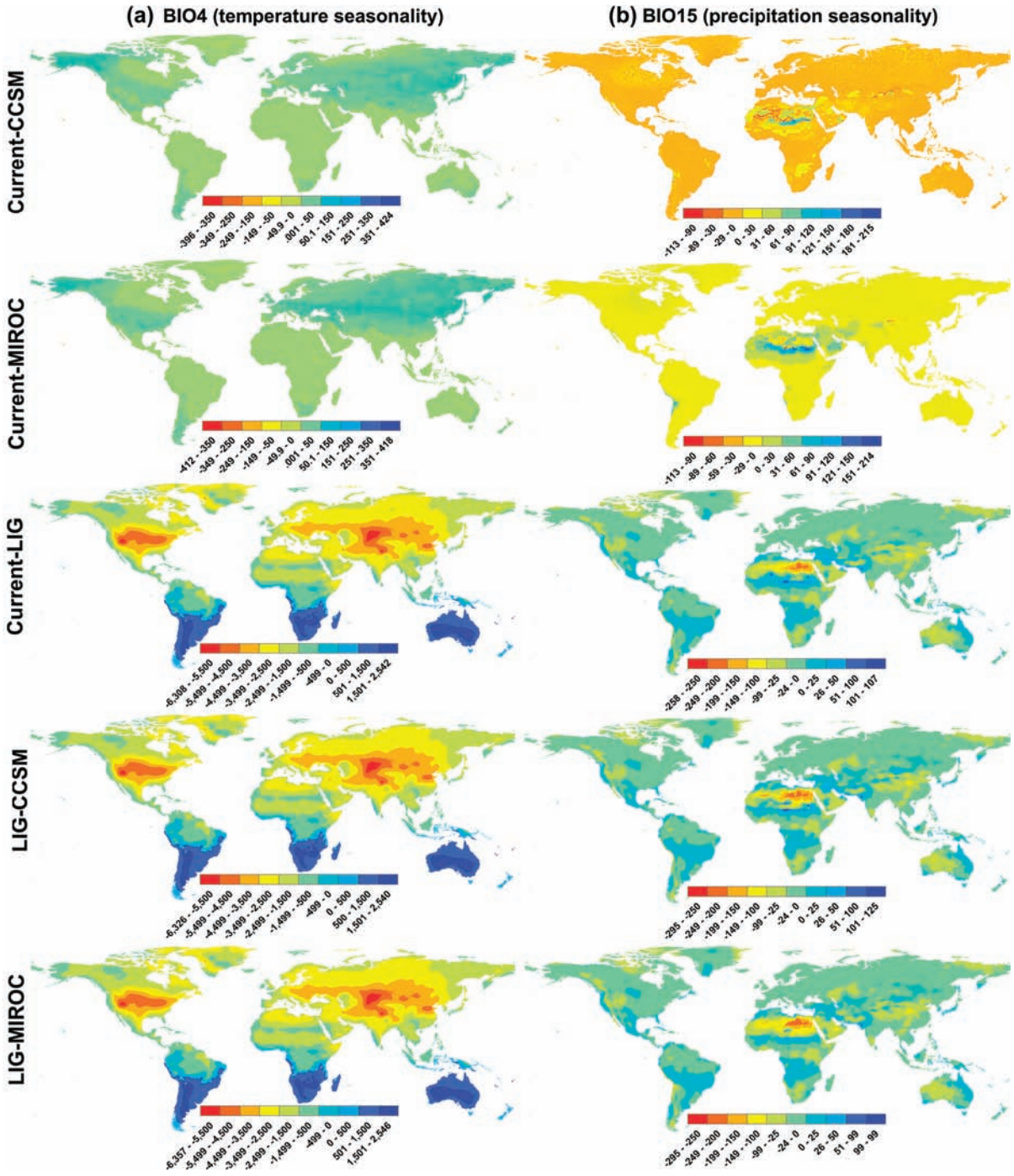

Figure 7. Climatic differences among three timeframes of current, LGM (under two atmospheric circulation models CCSM and MIROC) and LIG. Temperature (a) and precipitation seasonality (b) are shown. The values indicated here equal the values of each climate variable in the first scenario minus the second one as in Fig. 6.

3.6 Ma ago onwards massively affected the Chinese mountain systems at the eastern QTP margins (Li et al. 1996, Li and Fang 1999, Sun et al. 2011) and led to further intensification of winter monsoons and aridification along with an expansion of the Loess Plateau (An et al. 2001, Zheng et al. 2004). Even though the peculiarities of regional climate regimes in SE Asia (compared to other regions at similar latitudes) were presumably already established long before the onset of the Pleistocene, they were maintained and possibly even intensified under the impact of even late glacial cycles. For example, the fossil record of mollusks provided evidence of three major events of increased intensity of Asian summer monsoons at the eastern QTP margin during the last glacial cycles from 500 ka ago onwards (Rousseau et al. 1999). Generally, our ENMs showed that this region experienced a climate shift towards drier conditions and stronger seasonality and to more extreme temperatures of the coldest months particularly during the LIG. Apparently, Pleistocene climate change had a more drastic effect on temperature and precipitation regimes in southern China than in adjacent regions,

which might explain unusual paleo-distribution patterns of our target species and other SE Asian bird species, too.

Although the maximum temperature of the warmest month (BIO5) showed the frequently observed pattern from Europe and North America (LIG > current > LGM), the minimum temperature of the coldest month (BIO6) showed a deviating pattern in southern and western China (current > LGM > LIG) from Europe and North America (current > LIG > LGM; Supplementary material Appendix 1, Fig. A3). Therefore, the predicted relatively lower mean temperature of the LIG in east Asia should be more strongly related to the even lower temperature of the coldest months in a year. Finally, it is noteworthy that LGM scenarios inferred from different models (CCSM and MIROC) are not fully congruent with those from our study region (southern China). Differences among predicted LGM distributions might therefore simply be due to differences among extracted climatic-variable sets under the two different models. Further studies on improving the accuracy of reconstructed past climates is essential to explore the uncommon 'pre-LGM expansion' species distribution pattern in east Asia.

Acknowledgements – This study was supported by the National Natural Sciences Foundation of China (31301886). Travel funding for initial joint discussion and co-operation on this paper was provided by Deutsche Forschungsgemeinschaft (PA 1818/3-1). We sincerely thank Huw Lloyd his helpful comments and English writing improvements on the original version of the manuscript.

References

Allouche, O., Tsoar, A. and Kadmon, R. 2006. Assessing the accuracy of species distribution models: prevalence, kappa and the true skill statistic (TSS). – J. Appl. Ecol. 43: 1223–1232.

An, Z., Kutzbach, J. E., Prell, W. L. and Porter, S. C. 2001. Evolution of Asian monsoons and phased uplift of the Himalaya–Tibetan plateau since Late Miocene times. – Nature 411: 62–66.

Anderson, R. P. and Raza, A. 2010. The effect of the extent of the study region on GIS models of species geographic distributions and estimates of niche evolution: preliminary tests with montane rodents (genus *Nephelomys*) in Venezuela. – J. Biogeogr. 37: 1378–1393.

Araújo, M. B. and New, M. 2007. Ensemble forecasting of species distributions. – Trends Ecol. Evol. 22: 42–47.

Barve, N., Barve, V., Jiménez-Valverde, A., Lira-Noriega, A., Maher, S. P., Peterson, A. T., Soberón, J. and Villalobos, F. 2011. The crucial role of the accessible area in ecological niche modeling and species distribution modeling. – Ecol. Model. 222: 1810–1819.

Beheregaray, L. B. 2008. Twenty years of phylogeography: the state of the field and the challenges for the Southern Hemisphere. – Mol. Ecol. 17: 3754–3774.

Colwell, R. K., Brehm, G., Cardelús, C. L., Gilman, A. C. and Longino, J. T. 2008. Global warming, elevational range shifts, and lowland biotic attrition in the wet tropics. – Science 322: 258–261.

Dai, C., Zhao, N., Wang, W., Lin, C., Gao, B., Yang, X., Zhang, Z. and Lei, F. 2011. Profound climatic effects on two east Asian black-throated tits (Ave: Aegithalidae), revealed by ecological niche models and phylogeographic analysis. – PLoS One 6: e29329.

Dincă, V., Dapporto, L. and Vila, R. 2011. A combined genetic-morphometric analysis unravels the complex biogeographical history of *Polyommatus icarus* and *Polyommatus celina* common blue butterflies. – Mol. Ecol. 20: 3921–3935.

Elith, J. and Leathwick, J. R. 2009. Species distribution models: ecological explanation and prediction across space and time. – Annu. Rev. Ecol. Evol. Syst. 40: 677–697.

Elith, J., Graham, C. H., Anderson, R. P., Dudik, M., Ferrier, S., Guisan, A., Hijmans, R. J., Huettmann, F., Leathwick, J. R., Lehmann, A., Li, J., Lohmann, L. G., Loiselle, B. A., Manion, G., Moritz, C., Nakamura, M., Nakazawa, Y., Overton, J. M., Peterson, A. T., Phillips, S. J., Richardson, K., Scachetti-Pereira, R., Schapire, R. E., Soberon, J., Williams, S., Wisz, M. S. and Zimmermann, N. E. 2006. Novel methods improve prediction of species' distributions from occurrence data. – Ecography 29: 129–151.

Elith, J., Kearney, M. and Phillips, S. J. 2010. The art of modelling range-shifting species. – Methods Ecol. Evol. 1: 330–342.

Favre, A., Päckert, M., Pauls, S. U., Jähning, S. C., Uhl, D., Michalak, I. and Muellner-Riehl, A. N. 2014. The role of the uplift of the Qinghai-Tibetan Plateau for the evolution of Tibetan biotas. – Biol. Rev. 90: 236–253.

Fielding, A. H. and Bell, J. F. 1997. A review of methods for the assessment of prediction errors in conservation presence/absence models. – Environ. Conserv. 24: 38–49.

Freeman, E. A. and Moisen, G. 2008. PresenceAbsence: an R package for presence absence analysis. – J. Stat. Softw. 23: 1–31.

Guo, Z. T., Sun, B., Zhang, Z. S., Peng, S. Z., Xiao, G. Q., Ge, J. Y., Hao, Q. Z., Qiao, Y. S., Liang, M. Y., Liu, J. F., Yin, Q. Z. and Wie, J. J. 2008. A major reorganization of Asian climate regime by the early Miocene. – Clim. Past 4: 153–174.

Hewitt, G. 2000. The genetic legacy of the Quaternary ice ages. – Nature 405: 907–913.

Hewitt, G. M. 1996. Some genetic consequences of ice ages, and their role in divergence and speciation. – Biol. J. Linn. Soc. 58: 247–276.

Hijmans, R. J., Cameron, S. E., Parra, J. L., Jones, P. G. and Jarvis, A. 2005. Very high resolution interpolated climate surfaces for global land areas. – Int. J. Climatol. 25: 1965–1978.

Hijmans, R. J., Phillips, S., Leathwick, J. and Elith, J. 2011. dismo. Species distribution modeling. – R package ver. 0.5–17.

Huang, Z., Liu, N., Liang, W., Zhang, Y., Liao, X., Ruan, L. and Yang, Z. 2010. Phylogeography of Chinese bamboo partridge, *Bambusicola thoracica thoracica* (Aves: Galliformes) in south China: inference from mitochondrial DNA control-region sequences. – Mol. Phylogenet. Evol. 56: 273–280.

Jiménez-Valverde, A. and Lobo, J. M. 2007. Threshold criteria for conversion of probability of species presence to either-or presence–absence. – Acta Oecol. 31: 361–369.

Jiménez-Valverde, A., Peterson, A. T., Soberón, J., Overton, J. M., Aragón, P. and Lobo, J. M. 2011. Use of niche models in invasive species risk assessments. – Biol. Invasions 13: 2785–2797.

Kozak, K. H., Graham, C. H. and Wiens, J. J. 2008. Integrating GIS-based environmental data into evolutionary biology. – Trends Ecol. Evol. 23: 141–148.

Lait, L. and Burg, T. 2013. When east meets west: population structure of a high-latitude resident species, the boreal chickadee (*Poecile hudsonicus*). – Heredity 111: 321–329.

Lait, L. A., Friesen, V. L., Gaston, A. J. and Burg, T. M. 2012. The post-Pleistocene population genetic structure of a western North American passerine: the chestnut-backed chickadee *Poecile rufescens*. – J. Avian Biol. 43: 541–552.

Lei, F. and Lu, T. 2006. China endemic birds. – Science Press, Beijing, China.

Levsen, N. D., Tiffin, P. and Olson, M. S. 2012. Pleistocene speciation in the genus *Populus* (Salicaceae). – Syst. Biol. 61: 401–412.

Li, J. and Fang, X. M. 1999. Uplift of the Tibetan Plateau and environmental changes. – Chinese Sci. Bull. 44: 2217–2224.

Li, J., Fang, X., Ma, H., Zhu, J. J., Pan, B. T. and Chen, H. L. 1996. Geomorphological and environmental evolution in the upper reaches of the Yellow River during the late Cenozoic. – Sci. China Ser. D 39: 380–390.

Li, S. H., Li, J. W., Han, L. X., Yao, C. T., Shi, H., Lei, F. M. and Yen, C. 2006. Species delimitation in the hwamei *Garrulax canorus*. – Ibis 148: 698–706.

Lu, N., Jia, C.-X., Lloyd, H. and Sun, Y.-H. 2012a. Species-specific habitat fragmentation assessment, considering the ecological niche requirements and dispersal capability. – Biol. Conserv. 152: 102–109.

Lu, N., Jing, Y., Lloyd, H. and Sun, Y.-H. 2012b. Assessing the distributions and potential risks from climate change for the Sichuan jay (*Perisoreus internigrans*). – Condor 114: 365–376.

Manthey, J., Klicka, J., Spellman, G. and Larson, G. 2012. Is gene flow promoting the reversal of pleistocene divergence in the mountain chickadee (*Poecile gambeli*)? – PLoS One 7: e49218.

Marmion, M., Parviainen, M., Luoto, M., Heikkinen, R. K. and Thuiller, W. 2009. Evaluation of consensus methods in predictive species distribution modelling. – Divers. Distrib. 15: 59–69.

Nogués-Bravo, D. 2009. Predicting the past distribution of species climatic niches. – Global Ecol. Biogeogr. 18: 521–531.

Otto-Bliesner, B. L., Marshall, S. J., Overpeck, J. T., Miller, G. H. and Hu, A. 2006. Simulating Arctic climate warmth and icefield retreat in the last interglaciation. – Science 311: 1751–1753.

Owens, H. L., Campbell, L. P., Dornak, L. L., Saupe, E. E., Barve, N., Soberón, J., Ingenloff, K. K., Lira-Noriega, A., Hensz, C. M., Myers, C. E. and Peterson, A. T. 2013. Constraints on interpretation of ecological niche models by limited environmental ranges on calibration areas. – Ecol. Model. 263: 10–18.

Peterson, A. T. 2011. Ecological niche conservatism: a time-structured review of evidence. – J. Biogeogr. 38: 817–827.

Peterson, A. T. and Nakazawa, Y. 2008. Environmental data sets matter in ecological niche modelling: an example with *Solenopsis invicta* and *Solenopsis richteri*. – Global Ecol. Biogeogr. 17: 135–144.

Peterson, A. T., Lash, R. R., Carroll, D. S. and Johnson, K. M. 2006. Geographic potential for outbreaks of Marburg hemorrhagic fever. – Am. J. Trop. Med. Hyg. 75: 9.

Peterson, A. T., Papeş, M. and Eaton, M. 2007. Transferability and model evaluation in ecological niche modeling: a comparison of GARP and MaxEnt. – Ecography 30: 550–560.

Phillips, S. J. and Dudík, M. 2008. Modeling of species distributions with MaxEnt: new extensions and a comprehensive evaluation. – Ecography 31: 161–175.

Phillips, S. J., Anderson, R. P. and Schapire, R. E. 2006. Maximum entropy modeling of species geographic distributions. – Ecol. Model. 190: 231–259.

Potts, A. J., Hedderson, T. A. and Cowling, R. M. 2013a. Testing large scale conservation corridors designed for patterns and processes: comparative phylogeography of three tree species. – Divers. Distrib. 19: 1418–1428.

Potts, A. J., Hedderson, T. A., Franklin, J. and Cowling, R. M. 2013b. The Last Glacial Maximum distribution of South African subtropical thicket inferred from community distribution modelling. – J. Biogeogr. 40: 310–322.

Qu, Y., Luo, X., Zhang, R., Song, G., Zou, F. and Lei, F. 2011. Lineage diversification and historical demography of a montane bird *Garrulax elliotii* – implications for the Pleistocene evolutionary history of the eastern Himalayas. – BMC Evol. Biol. 11: 174.

Supplementary material (Appendix JAV-00590 at <www.avianbiology.org/readers/appendix>). Appendix 1.

Rousseau, D. D., Wu, N., Pei, Y. and Li, F. 1999. Three exceptionally strong east-Asian summer monsoon events during glacial times in the past 470 kyr. – Clim. Past 5: 157–169.

Schoener, T. W. 1968. The *Anolis* lizards of Bimini: resource partitioning in a complex fauna. – Ecology 49: 704–726.

Shaner, P. J. L., Tsao, T. H., Lin, R. C., Liang, W., Yeh, C. F., Yang, X. J., Lei, F.-M., Zhou, F., Yang, C.-C., Hung, L. M., Hsu, Y.-C. and Li, S.-H. 2015. Climate niche differentiation between two passerines despite ongoing gene flow. – J. Anim. Ecol. doi: 10.1111/1365–2656.12331

Sun, B. N., Wu, J. Y., Liu, Y. S., Ding, S. T., Li, X. C., Xie, S. P., Yan, D. F. and Lin, Z. C. 2011. Reconstructing Neogene vegetation and climates to infer tectonic uplift in western, Yunnan, China. – Palaeogeogr. Palaeoclimatol. Palaeoecol. 304: 328–336.

Sun, Y., Li, L., Li, L., Zou, J. and Liu, J. 2014. Distributional dynamics and interspecific gene flow in *Picea likiangensis* and *P. wilsonii* triggered by climate change on the Qinghai-Tibet Plateau. – J. Biogeogr. 42: 475–484.

Svenning, J.-C., Fløjgaard, C., Marske, K. A., Nógues-Bravo, D. and Normand, S. 2011. Applications of species distribution modeling to paleobiology. – Quat. Sci. Rev. 30: 2930–2947.

VanDerWal, J., Shoo, L. P., Graham, C. and Williams, S. E. 2009. Selecting pseudoabsence data for presence-only distribution modeling: how far should you stray from what you know? – Ecol. Model. 220: 589–594.

Waltari, E., Hijmans, R. J., Peterson, A. T., Nyári, S., Perkins, S. L. and Guralnick, R. P. 2007. Locating Pleistocene refugia: comparing phylogeographic and ecological niche model predictions. – PLoS One 2: e563.

Wang, W., Mckay, B. D., Dai, C., Zhao, N., Zhang, R., Qu, Y., Song, G., Li, S. H., Liang, W. and Yang, X. 2013. Glacial expansion and diversification of an east Asian montane bird, the green-backed tit (*Parus monticolus*). – J. Biogeogr. 40: 1156–1169.

Warren, D. L., Glor, R. E. and Turelli, M. 2008. Environmental niche equivalency versus conservatism: quantitative approaches to niche evolution. – Evolution 62: 2868–2883.

Warren, D. L., Glor, R. E. and Turelli, M. 2010. ENMTools: a toolbox for comparative studies of environmental niche models. – Ecography 33: 607–611.

Wilson, J. S. and Pitts, J. P. 2012. Identifying Pleistocene refugia in North American cold deserts using phylogeographic analyses and ecological niche modelling. – Divers. Distrib. 18: 1139–1152.

Xiangyu, J.-G., Yang, L. and Zhang, Y.-P. 2000. Sequence divergence between *Chrysolophus amherstiae* and *Chrysolophus pictus*. – Hereditas 22: 225–228.

Ye, Z., Zhu, G., Chen, P., Zhang, D. and Bu, W. 2014. Molecular data and ecological niche modeling reveal the Pleistocene history of a semi-aquatic bug (*Microvelia douglasi douglasi*) in east Asia. – Mol. Ecol. 23: 3080–3096.

Zhang, Y.-P., Chen, X. and Shi, L. 1991. Polymorphism in the mtDNA of three species of pheasants. – Zool. Res. 12: 387–392.

Zhao, N., Dai, C., Wang, W., Zhang, R., Qu, Y., Song, G., Chen, K., Yang, X., Zou, F. and Lei, F. 2012. Pleistocene climate changes shaped the divergence and demography of Asian populations of the great tit *Parus major*: evidence from phylogeographic analysis and ecological niche models. – J. Avian Biol. 43: 297–310.

Zheng, H., Powell, C. McA., Rea, D. K., Wang, J. and Wang, P. 2004. Late Miocene and mid-Pliocene enhancement of the east Asian monsoon as viewed from the land and sea. – Global Planet Change 41: 147–155.